The effect of the degree of mixing on the partially-premixed flame speed

Boulanger, J.; Liu, F.; Jiang, L.-Y.

Publisher's version / Version de l'éditeur:

2007 Spring Technical Meeting Combustion Institute/Canadian Section, Session G, Paper 7, pp. 1-6, 2007

THE EFFECT OF THE DEGREE OF MIXING ON THE PARTIALLY-PREMIXED FLAME SPEED

J. BOULANGER*, F. LIU[1], and L.-Y. JIANG

Gas Turbine Laboratory / IAR
[1]ICPET
National Research Council, Ottawa, ON

ABSTRACT

A relationship between the partially-premixed deflagration speed and the local degree of mixing was derived based on simple scaling laws. The results are validated by comparison with direct numerical simulations of the primitive equations. The correct trend is observed regarding the decrease of speed from the planar premixed deflagration down to the diffusion flame quenching with the narrowing of the local mixing-layer. Satisfactory agreements are also obtained considering the increase in the robustness of the flame with asymmetry of its tip.

INTRODUCTION

Phillips, [1], who reported the first observation of a triple-flame, was able to reveal a critical property of Partially-Premixed Flames (PPF): the speed is influenced by the thickness of the mixing-layer in which it is established. Narrowing the mixing-layer reduces the quality of mixing and makes the flame slow. Studies reported in the literature investigate relatively well mixed cases only, [2, 3], and view the flame front as a collection of non-interconnected flamelets. Buckmaster, [4], provides a description of the edge-flame based on the 1-D Diffusion Flame (DF) response. The whole system, which is in practice non-uniform along the local mixing-layer, is treated based on the response of the purely 1-D non-premixed situation. It is intended here to develop a correlation that would be valid for a broader range and including more realistic physical phenomena.

BASIC EQUATIONS

Combustion is simplified as a one-step irreversible reaction, in usual notations ($i = F$ or O for fuel or oxidizer species, respectively):

$$\dot{\omega} = -\frac{\rho\dot{\omega}_i}{\nu_i W_i} = A\left(\frac{\rho Y_O}{W_O}\right)^{\nu_O}\left(\frac{\rho Y_F}{W_F}\right)^{\nu_F} e^{-\frac{T_a}{T}} \tag{1}$$

*Building M-10, Room 104, 1200 Montréal Road, Ottawa, K1A 0R6, Ontario, Canada. Ph.: (613) 949 7687. Fx: (613) 952 7677. E-mail: Joan.Boulanger@nrc-cnrc.gc.ca

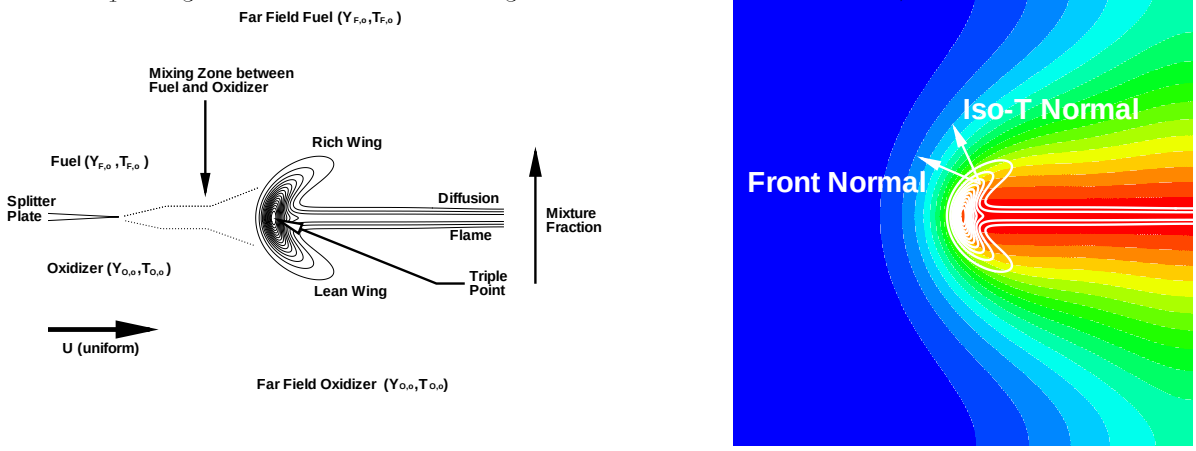

Figure 1: Left: configuration. Right: rotation laws of the normal to the flame front and the normal to the iso-T.

The mixture fraction is given by:

$$Z = \frac{\Phi Y_F/Y_{F,o} - Y_O/Y_{O,o} + 1}{1+\Phi} \qquad \text{where} \qquad \Phi = \frac{\nu_O W_O Y_{F,o} Le_O}{\nu_F W_F Y_{O,o} Le_F} \tag{2}$$

Z is linear in the spanwise direction and uniform in the streamwise direction. $Z_s = 1/(1+\Phi)$ is the stoichiometric mixture fraction and Z_a the composition maximizing the reaction rate, where the flame tip stabilizes.

The transport equations for species and temperature are written in usual notations:

$$\frac{D\rho Y_i}{Dt} - \nabla\cdot\left(\rho\frac{D_T}{Le_i}\vec{\nabla}Y_i\right) = \rho\dot{\omega}_i \tag{3a}$$

$$\frac{D\rho C_p T}{Dt} - \nabla\cdot\left(\rho C_p D_T\vec{\nabla}T\right) = -Q\rho\dot{\omega}_F \tag{3b}$$

From dimensional analysis [5], a reference length is given by (S_L is the PPF tip speed, the quantity to be sought):

$$\delta_L = \frac{\lambda}{C_p(\rho S_L)} \tag{4}$$

The species feeding free stream mass fractions, the jump in temperature, and the density ρ, heat C_p, conductivity λ in the flame at stoichiometry provide normalizing references to recast Eqs 3. The superscript $^+$ will be used to identify non-dimensional variables.

The non-dimensional temperature source term is thus defined as:

$$\dot{\omega}^+ = Da Y_F^{+\nu_F} Y_O^{+\nu_O} e^{-\beta\frac{1-T^+}{1-\alpha(1-T^+)}} \tag{5}$$

where the propagation-based Damköhler number is given as:
$Da = A\nu_F\frac{Le_F}{Z_s}(\rho^+\rho_s)^{\nu_F+\nu_O}(Y_{F,o}/W_F)^{\nu_F-1}(Y_{O,o}/W_O)^{\nu_O}\frac{\lambda_s/C_p}{(\rho S_L)^2}e^{-\beta/\alpha}$, the Zeld'ovitch parameter $\beta = \alpha(T_a/T_s)$ and the heat release rate $\alpha = (T_s - T_o(Z_s))/T_s$.

At the leading edge of a stabilized flame, and after the introduction of the Howarth-Dorodnitzyn transformation and the Chapman approximation, Eqs 3a and 3b become:

$$-\nabla Y_i^+\Big|_{\vec{n}} - Le_i^{-1}\Delta Y_i^+ = -\zeta_i\dot{\omega}^+ \tag{6a}$$

$$-\nabla T^+\Big|_{\vec{n}} - \Delta T^+ = \dot{\omega}^+ \tag{6b}$$

$\vec{n}$ is the normal to the flame front at the flame tip. $\zeta_i = \Phi^{\delta_{i,O}} Z_s / Le_i$.

The Laplacian is recast as:

$$\Delta T^+ = \vec{\nabla}||\vec{\nabla}T^+|| \cdot \frac{\vec{\nabla}T^+}{||\vec{\nabla}T^+||} + ||\vec{\nabla}T^+|| \overbrace{\nabla \cdot \frac{\vec{\nabla}T^+}{||\vec{\nabla}T^+||}}^{\text{(I)}} \tag{7}$$

Term (I) in the above equation is linked to the divergence of the normal to the iso-T. It does not exist for a planar front. In the case of a homogeneous curved front, it is simply related to the rotation of the flame front normal. In the present case, the front temperature is non-homogeneous. The rotation of the normalized vector in term (I) is more pronounced, Fig. 1(b), with the creation of an additional tangential term estimated as follows.

At the tip of the flame, $-\vec{\nabla}T^+/||\vec{\nabla}T^+||$ has no component tangential to the front. On the wings, at a distance scaling with the radius of curvature of the front $\mathcal{C}^{+-1}$, it is coarsely pointing to the side of the mixing-layer. This leads to the divergence along the tangential direction of the front of the order $\mathcal{C}^+$.

Thus, we have here an equivalent order of magnitude of the heat loss due to the curvature and the heat loss which creates the curvature. This is what is expected from common sense.

Equation 6b becomes, with the help of Eq. 7:

$$-\vec{\nabla}T^+\Big|_{\vec{n}} - \Delta T^+\Big|_{\vec{n}} - 2\mathcal{C}^+\vec{\nabla}T^+|_{\vec{n}} = \dot{\omega}^+ \tag{8}$$

INTERNAL ZONE

The temperature drop from its reference maximum value in the flame sheet is introduced as $T^+(Z_s) = 1 - \Gamma\varepsilon$, $\Gamma \approx 1$ and ε is a small parameter. In combustion, the high temperature dependence implies this drop must be small. This can only happen in a very thin sheet, slightly ahead of the burned gas, whose thickness $\delta_R = \varepsilon\delta_L$. This leads to coordinates magnifying to describe the reaction sheet structure: $\partial_{r^+} = \varepsilon^{-1}\partial_{r^*}$, $\mathcal{C}^+ = \varepsilon^{-1}\mathcal{C}^*$. r^+ is the distance along $\vec{n}$ from the centre of the flame tip osculatory circle.

Z, T^+, $\varepsilon\Gamma$ and Y_i^+ are linked together by enthalpy conservation. At the tip of the flame, Eq. 8 may be finally written at the leading order:

$$\frac{\partial^2\Gamma}{\partial r^{*2}} + 2\mathcal{C}^*\frac{\partial\Gamma}{\partial r^*} = Da\varepsilon^{\nu_F+\nu_O+1} Z_s^{\nu_F}(1-Z_s)^{\nu_O}\left(\Gamma + \frac{Z-Z_s}{Z_s(1-Z_s)\varepsilon}\right)^{\nu_F}\Gamma^{\nu_O}$$
$$\exp\left\{-\beta\varepsilon\left(\Gamma + (\gamma+1)\frac{Z-Z_s}{2Z_s(1-Z_s)\varepsilon}\right)\right\} \tag{9}$$

for $Z > Z_s$ (in a typical hydrocarbon flame, a slightly rich mixture maximizes the reaction rate and thus drives the tip stabilization).

The asymmetry factor of the diffusion flames, [6], is here recovered:

$$\gamma = 2\Big(Z_s\frac{Le_F C_p}{QY_{F,o}Z_s}(T_{O,o} - T_{F,o}) - 1\Big)(1-Z_s) + 1 \tag{10}$$

Across the diffusion layer, the infinitely fast chemistry temperature drop is sharper either on the rich side if $\gamma > 0$ or on the lean side if $\gamma < 0$. By shifting to the rich side, the flame tip also profits from the side with the weakest temperature slope.

To make the exponential argument a finite number in Eq. 9, the following scaling is required: $\beta\varepsilon \approx 1$.

By introducing the gradient of Z, the exponential argument of Eq. 9 becomes:

$$\Gamma + (\gamma+1)\frac{\beta\eta^+}{2Z_s(1-Z_s)}\mathcal{C}^{+-1}\theta \qquad \eta^+ = ||\vec{\nabla}Z|| \tag{11}$$

θ is the fraction of the spanwise dimension of the front where the heat release is close to its maximum ($\sim 90\%$ as a criterion). This defines the leading edge. A dimensional analysis based on an analogy with generic DF leads to $\theta \approx .2$ [7].

Thanks to the heat transfer from the tip to its neighbourhood, the extension of the leading reaction kernel where the temperature is *circa* equal to $1-\varepsilon$ competes with the Burke and Schumann solution:

$$(\gamma+1)\frac{\beta\eta^+}{2Z_s(1-Z_s)}\mathcal{C}^{+-1}\theta \approx \Gamma \approx 1 \tag{12}$$

which gives an estimate of the curvature:

$$\mathcal{C}^+ \approx (\gamma+1)\frac{\beta\eta^+}{10Z_s(1-Z_s)} \tag{13}$$

By aiming at incorporating heat transfers within the TF structure, the topology of the front is much better predicted than in the conventional TF theories which predict a really too narrow radius of curvature. Heat exchange within the structure is an integral fundamental TF phenomenon which cannot not be assumed as negligible. The interesting result at this step is the scaling of the curvature with the global temperature slope on the side of the flame. This is an expected result since the reaction rate is highly temperature dependent. The non-equilibrium solution has its maximum at Z_a instead of Z_s. Basing γ, Eq. 10, on Z_a instead of Z_s to estimate the tip curvature allows one to account for the global temperature slope in the actual flame configuration.

Integration of Eq. 9 from the burned gases towards the upstream of the reaction zone yields:

$$\varepsilon^{-1}\left[-\frac{\partial T^+}{\partial r^*}\right]_{-\infty}^{+\infty} - 2\mathcal{C}^*\varepsilon^{-1}[T^+]_{-\infty}^{+\infty} = [F(r^*)]_{-\infty}^{+\infty} = -\left(\frac{\partial T^+}{\partial r^+}\right)_{\mathcal{C}^{+-1}} + 2\mathcal{C}^+ \tag{14}$$

with the integrated reaction rate:

$$[F(r^*)]_{-\infty}^{+\infty} = \int_{-\infty}^{+\infty} dr^* Da\varepsilon^{\nu_F+\nu_O+1} Z_s^{\nu_F}(1-Z_s)^{\nu_O}(\Gamma + \beta\frac{Z_a - Z_s}{Z_s(1-Z_s)})^{\nu_F}\Gamma^{\nu_O} e^{-\left(\Gamma+(\gamma+1)\beta\frac{Z_a-Z_s}{2Z_s(1-Z_s)}\right)} \tag{15}$$

From this expression, the position of the flame tip is extracted as the location where the reaction rate is maximal:

$$Z_a = -\frac{\gamma}{1+\gamma}\frac{2Z_s(1-Z_s)}{\beta} + Z_s \qquad \nu_F = \nu_O = 1 \tag{16}$$

Through analogy with premixed flames, Eqs 14 and 15 provide a solution for Da from which the PPF speed is obtained:

$$S_L = S_L^o \frac{\sqrt{1 - \frac{\gamma}{\gamma+1} e^{\gamma}}}{1 + 2\mathcal{C}^+ - \left(\frac{\partial T^+}{\partial r^+}\right)_{\mathcal{C}^+ - 1}} \tag{17}$$

S_L^o is the stoichiometric premixed flame speed. The last term must match the external solution in the preheat zone to close the speed expression.

EXTERNAL ZONE

Behind the flame front, the temperature equals its equilibrium value at an order $1/\beta$. The region upstream of the flame is called the preheat zone. Despite the fact that Eq. 8 has been developed strictly in the flame region, it will also be used to estimate the temperature field in the preheat region. An *ad hoc* solution of the following form is proposed:

$$T^+ = e^{-r^+}\left(1 + \frac{1}{r^+}\right) e^{\frac{1}{\mathcal{C}^+}} \frac{1}{1 + \mathcal{C}^+} \tag{18}$$

It is an assembling of the solutions for weakly curved flames and for the Laplacian-dominated equation.

TEST AGAINST DIRECT NUMERICAL SIMULATIONS AND DISCUSSION

Direct simulations are conducted using a sixth-order steady-state incompressible DNS code, [8], over a square grid of 350×350 nodes. Grid independency has been checked. The size of the domain is chosen in such a way that it roughly corresponds to 20×20 stoichiometric unstrained planar premixed flame units. The transport coefficients are normalized and constant. The pre-exponential constant of the chemical term is chosen as: $Ae^{-\beta/\alpha} = \beta^3/4$, with $\beta = 15$. The reaction is second order. The computations are conducted for gradient magnitudes up to the presumed quenching value $\eta^+ = Z_s(1 - Z_s)$ [5]. For ease, the non-dimensionalization of η is approximated thanks to the stoichiometric planar premixed flame length.

Figure 2 shows the correlation between the normalized flame velocity S_L and the mixture fraction gradient η^+. It is seen that, with the increasing magnitude of the latter, the whole range of the partially-premixed regime is represented with good accuracy. When the flame is made asymmetrical by changing Z_s, the acceleration compared to the stoichiometric planar premixed flame is well retrieved, as well as the general trend *versus* η, showing that the location of the tip on the side with the weakest temperature drop helps reduce the curvature at the same time as maximizing the chemistry.

A correlation has been proposed in a simple form for the PPF speed with respect to non-mixing, based on a phenomenological analysis when the necessity of including new physical ingredients to accurately describe the PPF increases the mathematical complexity. It appears to be versatile and reliable for a wide range of configurations.

Dr. W. Wallace is gratefully acknowledged for his help in improving the final version of this communication.

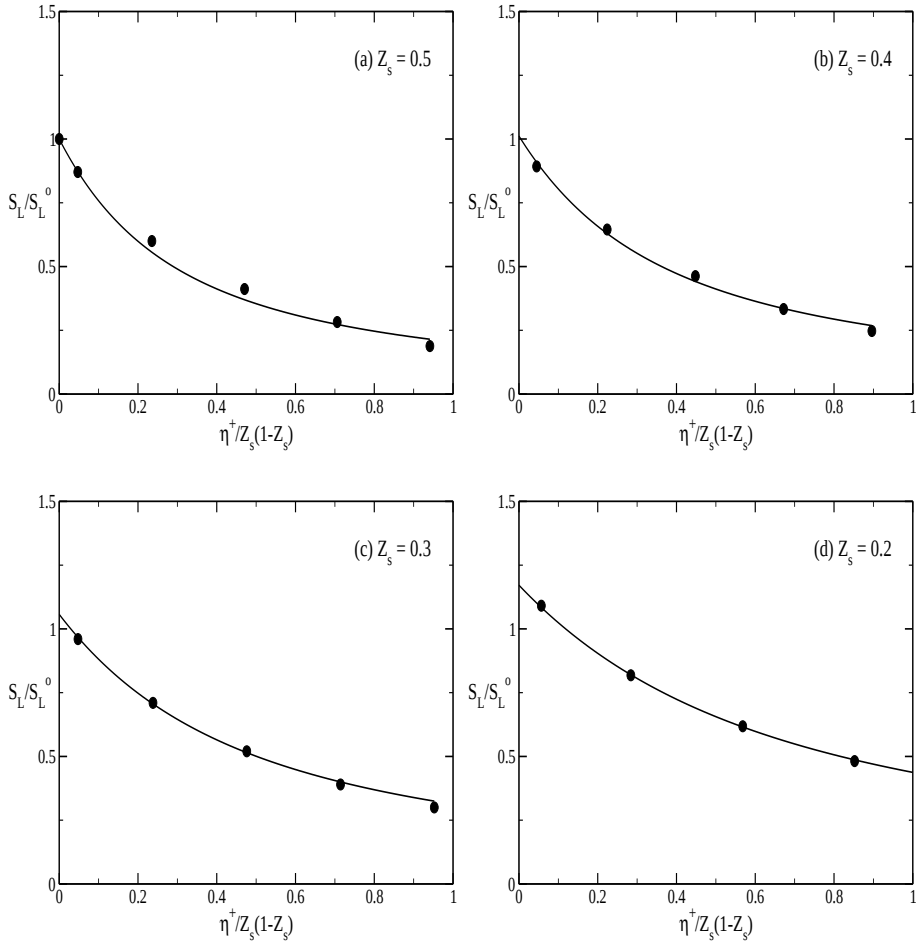

Figure 2: Response of the PPF velocity to the mixture fraction gradient. Filled circles: DNS. Line: analysis.

REFERENCES

[1] Phillips, H., volume 10, 1277–83, The Combustion Institute, Pittsburgh (1965).

[2] Dold, J., Combust. Flame, 76:71 (1989).

[3] Ghosal, S. and Vervisch, L., J. Fluid Mech., 415:227 (2000).

[4] Buckmaster, J., Prog. En. Comb. Sci., 28:435 (2002).

[5] Peters, N., *Length scales in laminar and turbulent flames*, volume 135, 155–82, AIAA, Washington DC, USA (1991).

[6] Liñán, A., Act. Astr., 1:1007 (1974).

[7] Boulanger, J., Liu, F., Smallwood, G. J., and Jiang, L.-Y., in *ICDERS Submitted* (2007).

[8] Boulanger, J. and Vervisch, L., Combust. Flame, 130:1 (2002).